
Scalable In-Context Q-Learning

Jinmei Liu¹ Fuhong Liu¹ Jianye HAO² Bo Wang¹ Huaxiong Li¹ Chunlin Chen¹ Zhi Wang¹

¹ Department of Control and Systems Engineering, Nanjing University, Nanjing, China

² College of Intelligence and Computing, Tianjin University, Tianjin, China

Abstract

Recent advancements in language models have demonstrated remarkable in-context learning abilities, prompting the exploration of in-context reinforcement learning (ICRL) to extend the promise to decision domains. Due to involving more complex dynamics and temporal correlations, existing ICRL approaches may face challenges in learning from suboptimal trajectories and achieving precise in-context inference. In the paper, we propose **Scalable In-Context Q-Learning (SICQL)**, an innovative framework that harnesses dynamic programming and world modeling to steer ICRL toward efficient reward maximization and task generalization, while retaining the scalability and stability of supervised pretraining. We design a prompt-based multi-head transformer architecture that simultaneously predicts optimal policies and in-context value functions using separate heads. We pretrain a generalized world model to capture task-relevant information, enabling the construction of a compact prompt that facilitates fast and precise in-context inference. During training, we perform iterative policy improvement by fitting a state value function to an upper-expectile of the Q-function, and distill the in-context value functions into policy extraction using advantage-weighted regression. Extensive experiments across a range of discrete and continuous environments show consistent performance gains over various types of baselines, especially when learning from suboptimal data. Our code is available at <https://github.com/NJU-RL/SICQL>.

1 Introduction

A longstanding goal of reinforcement learning (RL) is to learn from diverse experiences and generalize beyond its training environments, efficiently adapting to unseen situations, dynamics, or objectives [1, 2]. Recently, large language models (LLMs) [3, 4] have exhibited tremendous success in training large-scale transformer models on massive datasets to achieve remarkable in-context learning abilities, i.e., adapting to new tasks via prompt conditioning without any model updates [5, 6, 7]. Accordingly, in-context RL (ICRL) seeks to extend this promise to decision domains and has seen rapid progress in recent years [8]. Existing studies in offline settings contain two typical branches: algorithm distillation (AD) [9] and decision-pretrained transformer (DPT) [10], due to their simplicity and generality. They commonly employ cross-episode transitions as few-shot prompts and train transformer-based policies under supervised pretraining [11], followed by various improvements from model-based planning [12], hierarchical decomposition [13], importance weighting [14], etc [15, 16, 17].

Though, significant challenges may emerge when extending the promise of in-context learning from (self-) supervised learning to RL, since RL involves more complex dynamics and temporal correlations [18]. First, previous studies usually adopt a supervised pretraining paradigm, failing to utilize dynamic programming¹ offered by full RL algorithms to go beyond merely leveraging

¹In this paper, we use dynamic programming to indicate the fundamental characteristic of any RL algorithm relying on the Bellman-backup operation. It updates state (or state-action) values based on value estimates of successor states (or state-action pairs), i.e., bootstrapping [19]. We use dynamic programming and Q-learning interchangeably to refer to this fundamental property of RL.

collected data [20]. AD distills the entire learning history into a causal transformer, which can require long-horizon context and inherit suboptimal behaviors due to the gradual update rule [12]. DPT trains a transformer model to predict the optimal action given a query state and a prompt of interaction transitions, which relies on an oracle for optimal action labeling that can often be infeasible in practice [16]. Second, ICRL generally takes raw transitions as prompts that have many more tokens than a sentence and can be highly redundant.² Moreover, within transitions from offline datasets, the task information can be entangled with behavior policies, thus producing biased task inference at test time [22]. Hence, this type of prompt may be insufficient to precisely capture relevant information about decision tasks. The aforementioned limitations raise a key question: *Can we design a scalable ICRL framework using lightweight prompts that precisely capture task-relevant information, while unleashing the core potential of fundamental reward maximization to learn from suboptimal data?*

To tackle these challenges, we draw upon two basic properties inherent in full RL. First, classical RL algorithms learn a value function to backpropagate expected returns using dynamic programming updates, showing high stitching capacity, i.e., the ability to combine parts of suboptimal trajectories for finding globally optimal behaviors [19]. Naturally, the stitching property offers a compelling avenue for unleashing the potential of ICRL architectures, attaining substantial improvement over suboptimal data. Second, RL agents learn through active interactions with the outer world (environment) based on the Markov decision process (MDP) formulation. The world model (environment dynamics) [23] completely characterizes the underlying task, and is intrinsically invariant to behavior policies or collected datasets [24]. Hence, leveraging the world model holds promise for designing a lightweight prompt structure capable of precisely encoding task-relevant information.

Drawing inspiration from full RL, we propose **Scalable In-Context Q-Learning (SICQL)**, an innovative framework that harnesses dynamic programming and world modeling to steer ICRL toward efficient reward maximization and task generalization. First, we design a prompt-based multi-head transformer architecture to maintain scalability and parameter efficiency. The model simultaneously predicts optimal policies and in-context value functions using separate heads, given a task prompt and corresponding query inputs. Second, we pretrain a generalized world model to capture task-relevant information from the multi-task offline dataset, and use it to transform a small number of raw transitions into a lightweight prompt for fast and precise in-context inference. Finally, we perform iterative policy improvement by fitting a state value function to an upper-expectile of the Q-function, and distill the in-context value functions into policy extraction using advantage-weighted regression. This formulation allows for learning a policy to maximize the Q-values subject to an offline dataset constraint, while retaining the scalability and stability of the supervised pretraining paradigm.

In summary, our main contributions are threefold:

- We introduce dynamic programming to supervised ICRL architectures, unleashing its potential toward learning from suboptimal trajectories with efficient reward maximization.
- We design a lightweight prompt structure that leverages world modeling to accurately capture task-relevant information, enabling fast and precise in-context inference.
- We propose a scalable and parameter-efficient ICRL framework that integrates the advantages of RL and supervised learning paradigms. Comprehensive experiments validate our superiority over a range of baselines, especially when learning from suboptimal data.

2 Related Work

The concept of agents adapting their behaviors within the context without model updates builds on earlier work in meta-RL, notably RL² [25] that includes past interactions as inputs to an RNN-based policy. Recently, there has been a shift towards employing transformers to implement ICRL [8], driven by their proven ability to capture long-term dependencies and exhibit emergent in-context learning behaviors [5]. In online RL settings, AMAGO [26, 27] trains long-sequence transformers over entire rollouts with actor-critic learning to tackle in-context goal-conditioned problems, and [28] leverages the S4 (structured state space sequence) model’s ability to handle long-range sequences for ICRL tasks. In offline settings, two classical branches are AD [9] and DPT [10]. AD trains a causal transformer to

²In language communities, the prompts are concise and precise text instructions with rich semantic information, as texts or words naturally involve high-level concepts that describe entire semantic entities such as objects (nouns) and actions (verbs) [21].

autoregressively predict actions using preceding learning histories as context, while DPT predicts the optimal action based on a query state and a prompt of interaction transitions. Subsequent studies further increase their in-context learning capacities from various perspectives [12, 13, 15, 17, 29]. For example, IDT [13] designs a hierarchical structure of human decision-making, and DICI [12] incorporates model-based planning with a learned dynamics model. These approaches generally adopt a supervised paradigm and use raw transitions as prompts, while we harness dynamic programming for reward maximization and leverage world modeling to construct more efficient prompts.

DIT [14] and IC-IQL [16] are the most relevant to our work. DIT [14] also uses a weighted maximum likelihood estimation loss to train the transformer policy, where the weights are directly calculated from observed rewards in collected datasets. In contrast, we learn separate in-context value functions for computing advantage weights, enabling more stable and sample-efficient policy extraction. IC-IQL [16] integrates a Q-learning objective into AD. The policy network is updated by optimizing only its head, whereas the value function update propagates through both the head and the transformer backbone. In contrast, we train the whole multi-head transformer policy end-to-end, releasing the transformer’s scalability with a simplified pipeline. Also, we design a lightweight prompt structure to overcome the limitation of AD algorithms that require long training histories as context. Empirical results in Sec. 5 also demonstrate our superiority to these two baselines.

3 Preliminaries: In-Context Reinforcement Learning

We consider a multi-task offline RL setting, where tasks follow a distribution $M^i = \langle \mathcal{S}, \mathcal{A}, \mathcal{T}_i, \mathcal{R}_i, \gamma \rangle \sim P(M)$. Tasks share the same state-action spaces \mathcal{S}, \mathcal{A} , while differing in the reward function \mathcal{R} or transition dynamics \mathcal{T} . An offline dataset $\mathcal{D}^i = \sum_j (s_j^i, a_j^i, r_j^i, s_j^{i'})$ is collected by arbitrary behavior policies for each task out of a total of N training ones. The agent can only access the offline datasets $\{\mathcal{D}^i\}_{i=1}^N$ to train an in-context policy as $\pi_\theta(a^i | s^i; \beta^i)$, where β^i is a prompt that encodes task-relevant information. β can be the preceding learning history in AD and a sequence of transitions in DPT.

During testing, the trained policy is evaluated on unseen tasks sampled from $P(M)$ through direct interaction with the environment. With fixed policy parameters θ , all adaptations happen via the prompt/context β that is initially empty and gradually constructed from history interactions. As β evolves, the model revises its predictions in a manner analogous to the policy updates in conventional RL algorithms. The objective is to learn an in-context policy that maximizes the expected episodic return over test tasks as $J(\pi) = \mathbb{E}_{M \sim P(M)} [J_M(\pi)]$.

4 Method

In this section, we present **SICQL** (Scalable In-Context Q-Learning), an innovative ICRL framework that leverages dynamic programming and world modeling for efficient reward maximization and task generalization. Figure 1 illustrates the method overview. The algorithm pseudocodes are presented in Appendix B, and detailed implementations are given as follows

4.1 Prompt Construction via World Modeling

A key obstacle in RL generalization across tasks is how to accurately capture task-relevant information from offline datasets. In language communities, prompts consist of concise and precise text instructions rich in semantic information, as words inherently convey high-level concepts that represent entire semantic entities like objects (nouns) and actions (verbs) [21]. In contrast, ICRL approaches typically use a collection of raw state-action-reward transitions to infer the underlying task and identify what actions lead to good outcomes [10]. The resulting prompt has many more tokens than a sentence and can be highly redundant. For instance, the states in a trajectory change smoothly with minor local variations [30], and in sparse-reward scenarios, only a very small fraction of transition data contains valuable information [31]. Moreover, in offline RL settings, the task information can be entangled with behavior policies, leading to biased task inference at test time due to the change of behavior policies [22, 24]. Overall, the current type of prompt may be insufficient to achieve precise in-context task inference for ICRL.

To address this challenge, we aim to design a lightweight prompt structure capable of encoding precise information about decision tasks. RL agents learn by actively interacting with the external

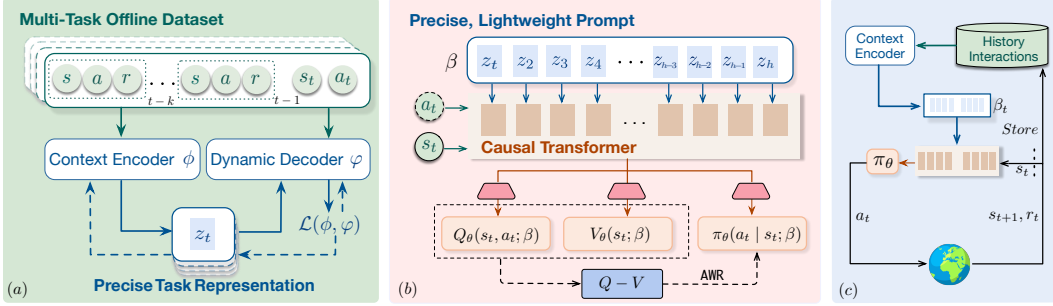


Figure 1: The overview of SICQL. (a) We pretrain a generalized world model to accurately capture task-relevant information from the multi-task offline dataset as in Eq. (2), and use the context encoder to transform a small number of raw transitions into a precise and lightweight prompt β as in Eq. (3). (b) We design a prompt-based multi-head transformer model that simultaneously predicts the optimal policy $\pi_\theta(a|s; \beta)$, the state value function $V_\theta(s; \beta)$, and Q-function $Q_\theta(s, a; \beta)$ using separate heads, given the task prompt β and corresponding query inputs (s or s, a). We learn V_θ by expectile regression as in Eq. (5), and use it to compute Bellman backups for training Q_θ as in Eq. (4). The in-context value functions are distilled into policy extraction using advantage-weighted regression as in Eq. (6). (c) Online testing by interacting with the environment. The prompt is initially empty and gradually constructed from history interactions using the pretrained context encoder.

environment, modeled as an MDP. The world model, representing environment dynamics [23], fully characterizes the underlying task and remains invariant to behavior policies or the datasets collected. Inspired by this fundamental property of RL, we pretrain a generalized world model to acquire task-relevant information from the multi-task offline dataset, and use it to transform raw transitions (s, a, r) into compact task representations z to construct the prompt.

The environment dynamics, i.e., the reward and state transition functions, can share some common structure across the task distribution. For each task M^i , we approximate its dynamics by a generalized world model P that is shared across tasks, defined as

$$P_i(r_t, s_{t+1}|s_t, a_t) \approx P(r_t, s_{t+1}|s_t, a_t; z_t^i), \quad \forall \text{ task } i. \quad (1)$$

As the true task identity is unknown, we infer task representation z_t^i from the agent’s k -step experience within task M^i as $\eta_t^i = (s_{t-k}, a_{t-k}, r_{t-k}, \dots, s_{t-1}, a_{t-1}, r_{t-1}, s_t, a_t)^i$. The intuition is that the true task belief can be inferred from the agent’s history interactions, similar to recent meta-RL studies [32, 33]. We use a context encoder E_ϕ to abstract recent k -step experiences into a task representation as $z_t^i = E_\phi(\eta_t^i)$, which is augmented into the input of a dynamics decoder D_φ to predict the instant reward and next state as $[\hat{r}_t, \hat{s}_{t+1}] = D_\varphi(s_t, a_t; z_t^i)$. Based on the assumption that tasks with similar contexts will behave similarly [34], our generalized world model can extrapolate meta-level knowledge across tasks by precisely capturing task-relevant information. The context encoder and dynamics decoder are jointly trained by minimizing the reward and state transition prediction error as

$$\mathcal{L}(\phi, \varphi) = \mathbb{E}_{\eta_t^i \sim M^i} \left[\mathbb{E}_{z_t^i \sim E_\phi(\eta_t^i)} [\| [r_t, s_{t+1}] - D_\varphi(s_t, a_t; z_t^i) \|^2] \right], \quad \forall \text{ task } i. \quad (2)$$

After proper pretraining, we freeze the generalized world model for prompt construction during policy training. At each training step, we sample a short h -step trajectory $[s_1, a_1, r_1, \dots, s_h, a_h, r_h]^i$ randomly from dataset \mathcal{D}^i , and use the pretrained context encoder E_ϕ to transform raw transitions in this trajectory into compact task representations as

$$\beta^i := [z_1, \dots, z_h]^i = E_\phi([s_1, a_1, r_1, \dots, s_h, a_h, r_h]^i), \quad \forall \text{ task } i. \quad (3)$$

Then, we construct a *lightweight* prompt β using the h -step task representation for fast and precise in-context inference, as opposed to AD algorithms that can require long training histories as context.

4.2 In-Context Q-Learning

The mainstream ICRL methods adopt a supervised learning routine to train transformer policies. However, they often lack the capacity for policy stitching, one of the fundamental abilities of the

full RL paradigm to learn optimal policies from suboptimal data [20]. This issue becomes more pronounced when the offline dataset consists solely of suboptimal trajectories, especially for pure imitation learning approaches that rely on an oracle for optimal action labeling, such as DPT. Classical RL algorithms learn a value function to backpropagate expected returns using dynamic programming updates, showcasing high stitching capacity that allows for not only leveraging collected data but also achieving substantial improvement beyond it [19]. Inspired by this, we harness the stitching property to offer a promising avenue for unleashing ICRL’s potential toward explicit reward maximization.

In-Context Value Functions. Following common practice in advanced offline RL algorithms [35, 36], we learn both a state value function V and an action value function Q . To maintain scalability and parameter efficiency, we design a multi-head transformer architecture to predict the policy and value functions using three separate heads. Let θ denote parameters of the integrated transformer model. The model outputs the policy $\pi_\theta(a|s; \beta)$, the state value $V_\theta(s; \beta)$, and the action value $Q_\theta(s, a; \beta)$, given the task prompt β and corresponding query inputs. The in-context Q-function is trained to minimize the Bellman bootstrapping error as

$$\mathcal{L}_Q(\theta) = \mathbb{E}_{(s_t^i, a_t^i, s_{t+1}^i) \sim \mathcal{D}^i} \left[\left(r(s_t^i, a_t^i) + \gamma V_\theta(s_{t+1}^i; \beta^i) - Q_\theta(s_t^i, a_t^i; \beta^i) \right)^2 \right], \quad \forall \text{ task } i. \quad (4)$$

The in-context state value function V_θ aims to fit an upper-expectile of the Q-function, and is trained to minimize an expectile regression loss as

$$\mathcal{L}_V(\theta) = \mathbb{E}_{(s_t^i, a_t^i) \sim \mathcal{D}^i} \left[L_2^\omega(Q_\theta(s_t^i, a_t^i; \beta^i) - V_\theta(s_t^i; \beta^i)) \right], \quad \forall \text{ task } i, \quad (5)$$

where $L_2^\omega(u) = |\omega - \mathbb{1}(u < 0)| \cdot u^2$ is an asymmetric loss function with a expectile parameter $\omega \in (0, 1)$, introduced in implicit Q-learning [35]. This form of expectile regression reduces the influence of $Q < V$ predictions by a factor of $1 - \omega$ while assigning more importance to $Q > V$ predictions by a factor of ω . In this way, we predict an upper-expectile of the temporal-difference target that approximates the maximum of $r(s_t^i, a_t^i) + \gamma Q_\theta(s_{t+1}^i, a_{t+1}^i; \beta^i)$ over actions a_{t+1}^i constrained to the dataset actions. The algorithm alternates between fitting the state value function with expectile regression and using it to compute Bellman backups for training the Q-function, performing efficient dynamic programming updates for multiple iterations.

In-Context Policy Extraction. The value function learning procedure learns an in-context approximation of optimal Q-functions across tasks, allowing for stitching suboptimal trajectories to discover globally optimal behaviors through value bootstrapping. Then, we distill the in-context value functions into policy extraction with advantage-weighted regression [37], a supervised learning style that uses a simple and convergent maximum likelihood loss function as

$$\mathcal{L}_\pi(\theta) = -\mathbb{E}_{(s_t^i, a_t^i) \sim \mathcal{D}^i} \left[\exp \left(\frac{1}{\lambda} (Q_\theta(s_t^i, a_t^i; \beta^i) - V_\theta(s_t^i; \beta^i)) \right) \cdot \log \pi_\theta(a_t^i | s_t^i; \beta^i) \right], \quad \forall \text{ task } i, \quad (6)$$

where $\lambda > 0$ is a temperature parameter. Using weights derived from in-context value functions, the objective is not merely to clone all behaviors from the dataset, but to learn a policy that maximizes the Q-values subject to a distribution constraint imposed by dataset actions. This formulation allows us to select and stitch the most optimal actions in the dataset, while retaining the scalability and stability of the supervised pretraining paradigm.

Finally, the backbone and three separate heads are jointly updated by the overall loss function as

$$\mathcal{L}(\theta) = \mathcal{L}_\pi(\theta) + \mathcal{L}_Q(\theta) + \mathcal{L}_V(\theta). \quad (7)$$

5 Experiments

We comprehensively evaluate the in-context learning capacity of SICQL on popular benchmarking domains across different dataset types. In general, we aim to answer the following questions:

- Can SICQL achieve consistent performance gain on few-shot generalization ability to unseen tasks compared to other strong baselines? (Sec. 5.1)
- How do the prompt construction via world modeling and the reward maximization via dynamic programming affect the in-context learning performance, respectively? (Sec. 5.2)
- Is SICQL robust to the quality of offline datasets and hyperparameters? (Sec. 5.3 and Sec. 5.4)

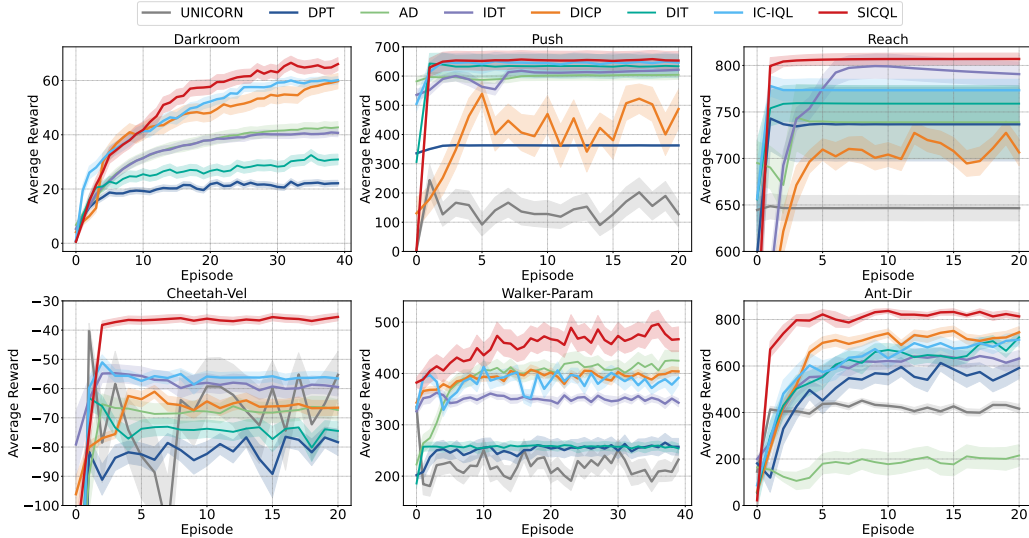


Figure 2: Few-shot evaluation return curves of SICQL and baselines on Mixed datasets.

Environments. We conduct experiments on three challenging benchmarks commonly used for evaluating meta-RL and ICRL algorithms with a multi-task setting: i) *DarkRoom* [9], a 2D discrete environment where the agent must locate an unknown goal within a 10×10 room, receiving a reward of 1 only when it reaches the goal. ii) The multi-task MuJoCo control [38], a well-established testbed that contains two environments where tasks differ in reward functions (*Cheetah-Vel* and *Ant-Dir*) and one environment where tasks differ in transition dynamics (*Walker-Param*). iii) The Meta-World ML1 benchmark suite [39], a popular robotic platform where a simulated Sawyer arm is designed to perform a wide range of 50 robotic manipulation tasks. We consider two environments of *Reach-v2* and *Push-v2*, where the robotics arm needs to reach a randomly assigned goal position in 3D space and push a block to a randomly placed target on a tabletop. For each environment, we sample tasks at random from the task distribution and split them into a training set M^{train} and a test set M^{test} . More details about evaluation environments are provided in Appendix C.

Pretraining Datasets. For *DarkRoom*, we use a noisy action selection strategy during dataset collection: with probability ϵ , the optimal policy is applied, and with probability $1-\epsilon$, a random policy is used. The value of ϵ is set to make sure that the average return in the pretraining dataset is less than 40% of the optimum, thus constructing a suboptimal dataset. We use Soft Actor-Critic (SAC) [40] for MuJoCo and Proximal Policy Optimization (PPO) [41] for Meta-World to train a single-task policy independently for collecting the dataset of each task. We construct two qualities of offline datasets: *Mixed* and *Medium*. More details on dataset construction are provided in Appendix D.

Baselines. We compare to six competitive ICRL approaches and one offline meta-RL method, including: 1) IC-IQL [16], 2) DIT [14], 3) DICP [12], 4) IDT [13], 5) AD [9], 6) DPT [10], and 7) UNICORN [42]. Details about these baselines are provided in Appendix E.

To ensure a fair comparison, we conduct a few-shot evaluation for all methods. During testing, the policy directly interacts with the environment for a few episodes with fixed policy parameters, conditioned on a prompt sampled from history interactions. The reported results represent the mean of 10 evaluation trials, with mean returns accompanied by 95% bootstrapped confidence intervals. Standard errors are also provided for the numerical results.

5.1 Main Results

The baselines typically work under the few-shot setting, since they rely on task prompts or warm-start data to infer task representations. We evaluate SICQL against these baselines in an aligned few-shot setting, where all methods utilize the same number of interaction trajectories for task inference. Figure 2 illustrates the evaluation return curves across various environments using *Mixed* datasets, and Table 1 summarizes the numerical results of converged performance. Across environments with

Table 1: Few-shot evaluation returns of SICQL and baselines on Mixed datasets, i.e., numerical results of converged performance from Figure 2.

Methods	Darkroom	Push	Reach	Cheetah-Vel	Walker-Param	Ant-Dir
UNICORN	/	127.69± 44.04	646.52± 13.60	-55.29± 7.90	232.23± 21.73	416.35± 18.29
DPT	22.12± 1.09	362.74± 1.91	736.72± 39.42	-78.35± 4.50	257.11± 16.36	591.31± 45.54
AD	42.72± 2.14	604.50± 15.52	738.96± 39.38	-67.37± 3.53	424.82± 19.23	215.01± 46.61
IDT	40.70± 1.44	621.58± 11.16	790.68± 13.01	-59.46± 3.10	343.01± 7.95	631.83± 35.29
DICP	59.76± 2.80	487.28± 66.33	706.46± 14.32	-66.53± 2.58	403.90± 8.09	745.05± 24.12
DIT	30.90± 1.96	633.58± 39.22	758.92± 19.13	-74.50± 3.24	253.94± 9.04	723.49± 27.36
IC-IQL	60.12± 1.33	646.08± 30.34	773.33± 11.79	-56.53± 1.98	391.38± 13.97	713.26± 27.23
SICQL	66.05± 2.37	653.04± 31.22	806.97± 6.35	-35.48± 1.33	466.72± 24.06	813.34± 14.12

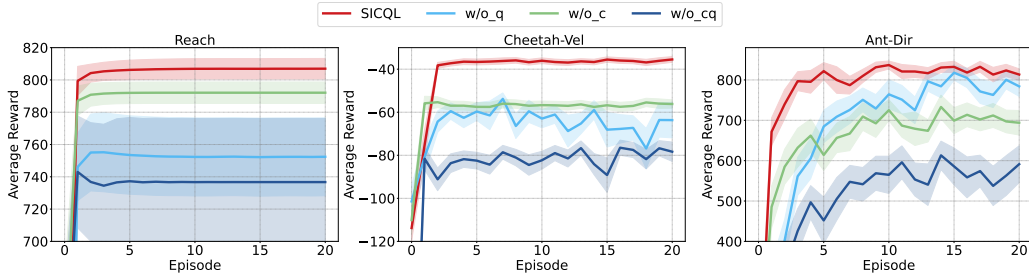


Figure 3: Few-shot evaluation return curves of SICQL and its ablations on Mixed datasets. w/o_c removes world modeling, w/o_q removes Q-learning, and w/o_cq removes both components.

Table 2: Few-shot evaluation returns of SICQL and its ablations on Mixed datasets, i.e., numerical results of converged performance from Figure 3.

Environments	w/o_cq	w/o_c	w/o_q	SICQL
Reach	736.72 ± 39.42	792.09 ± 6.66	752.41 ± 24.15	806.97 ± 6.35
Cheetah-Vel	-78.35 ± 4.50	-56.19 ± 1.94	-63.66 ± 8.26	-35.48 ± 1.33
Ant-Dir	591.31 ± 45.54	693.87 ± 30.41	784.07 ± 24.88	813.34 ± 14.12

varying reward functions and transition dynamics, SICQL consistently demonstrates superior data efficiency and higher asymptotic performance. In more complex environments such as Ant-Dir and HalfCheetah-Vel, the advantage of SICQL is more pronounced, highlighting its promising in-context learning abilities on challenging tasks. Moreover, SICQL generally exhibits lower variance during the testing phase, indicating both improved data efficiency and better training stability.

Notably, DPT yields suboptimal performance across most environments, underscoring the critical role of incorporating fundamental reward maximization into our framework. The significant improvement over DIT and IC-IQL also verifies that our method can provide a more efficient way for policy extraction with advantage-weighted regression or incorporating Q-learning objectives.

5.2 Ablation Study

To assess the respective contribution of each component, we compare SICQL with three ablations: (i) w/o_c, it removes the world modeling component and directly uses a trajectory of raw transitions to construct prompts; (ii) w/o_q, it removes the Q-learning component and learn in-context policies in a pure supervised paradigm; and (iii) w/o_cq, which removes both world modeling and Q-learning, reducing the model to the original DPT. In all ablations, the remaining structural components are kept identical to those in the full SICQL.

Figure 3 and Table 2 present the ablation results across representative environments. First, removing any individual component significantly degrades SICQL’s performance, highlighting the critical role of each module and their nontrivial integration. Second, ablating the world model leads to a notable performance drop, especially in complex environments like Ant-Dir, which emphasizes the

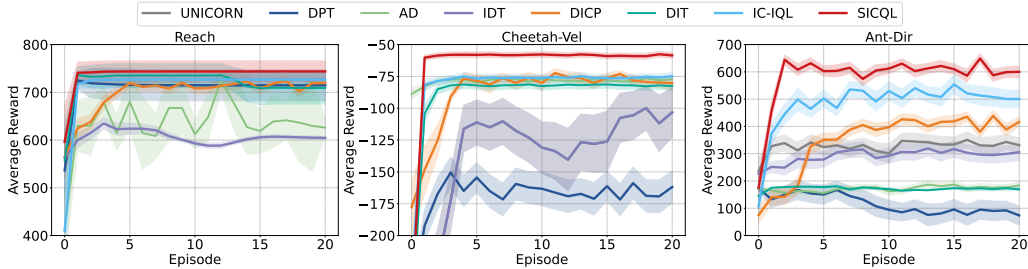


Figure 4: Few-shot evaluation return curves of SICQL and baselines on Medium datasets.

importance of world modeling for precise in-context inference. Third, removing the Q-learning component reduces performance, underscoring its role in leveraging suboptimal data for efficient policy refinement. Integrating Q-learning allows SICQL to improve policies from noisy or inferior trajectories, enhancing the stitching ability for reward maximization. Finally, removing both the world model and Q-learning results in the greatest performance degradation, reducing the model to a baseline form of behavioral cloning that fails to generalize in complex tasks. This confirms the indispensability of both components for robust performance in ICRL. Overall, the ablation result validates SICQL’s effectiveness in harnessing both world modeling and Q-learning for efficient reward maximization and generalization across tasks.

5.3 Robustness to the Quality of Offline Datasets

To evaluate SICQL’s robustness to data quality, we conduct experiments on Medium datasets that only contain suboptimal data. Figure 4 and Table 3 show SICQL’s performance against baselines on representative environments. SICQL consistently outperforms all baselines, especially in complex environments such as Cheetah-Vel and Ant-Dir, showcasing its superiority when learning from suboptimal trajectories. Notably, many baselines converge to suboptimal policies using imperfect data, especially for pure imitation learning methods like DPT. This again highlights our advantage of using Q-learning to not only simply leverage collected data, but also to combine parts of suboptimal trajectories for finding globally optimal behaviors. Overall, the above results, together with those in Sec. 5.1, confirm the robustness of our method to dataset quality.

Table 3: Few-shot evaluation returns of SICQL and baselines using Medium datasets, i.e., numerical results of converged performance.

Methods	Reach	Cheetah-Vel	Ant-Dir
UNICORN	366.53± 1.98	-103.23± 19.35	331.23± 25.75
DPT	714.70± 32.51	-161.88± 12.61	73.72± 34.71
AD	626.24± 19.08	-77.30± 2.06	183.51± 11.82
IDT	604.49± 3.54	-103.23± 19.35	305.50± 30.20
DICP	719.54± 10.20	-80.34± 5.82	416.58± 16.80
DIT	709.07± 33.65	-82.61± 3.15	169.22± 5.18
IC-IQL	726.68± 15.61	-74.88± 2.78	500.20± 31.49
SICQL	743.72± 22.15	-58.48± 2.32	600.18± 21.46

5.4 Hyperparameter Analysis

The temperature parameter λ in Eq.(6) plays a crucial role in balancing the trade-off between behavior cloning and the greedy pursuit of high Q-values. We conduct experiments to analyze the influence of λ on SICQL’s performance. Table 4 present the few-shot ablation results across representative domains with varying values of λ . A smaller λ will make the distribution of advantage weights $\exp(\frac{1}{\lambda})(Q - V)$ less uniform, leading to more exploitation of Q-learning. As λ decreases from 1.0, the performance of SICQL can be greatly improved, highlighting the essentiality of harnessing Q-learning to steer ICRL architectures toward fundamental reward maximization. In practice, a small value of $\lambda = 0.01$ or $\lambda = 0.001$ leads to a satisfactory performance. The result further confirms the effectiveness and necessity of our in-context Q-learning.

Table 4: Few-shot results of SICQL’s performance with varying λ on Mixed datasets.

λ	Reach	Cheetah-Vel	Ant-Dir
1.0	765.99± 17.93	-99.16± 4.00	486.23± 30.98
0.1	796.42± 7.20	-46.54± 2.37	749.00± 19.55
0.01	799.29± 2.77	-46.56± 3.08	813.34± 14.12
0.001	806.97± 6.35	-35.48± 1.33	767.55± 19.89

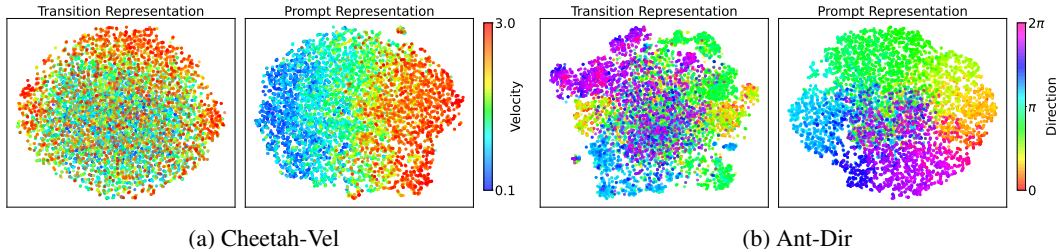


Figure 5: t-SNE visualization on Cheetah-Vel and Ant-Dir, where tasks differ in target velocities of $[0.1, 3.0]$ and target directions of $[0, 2\pi]$. Data representations of raw transitions (s, a, r, s') and precise prompts β from a distribution of tasks are mapped into rainbow-colored points.

In prompt construction, the task representation z_t^i is inferred from the agent’s k -step experience η_t^i as $z_t^i \sim E_\phi(\eta_t^i)$. The step k plays a crucial role in capturing task-relevant information. We conduct experiments to investigate the impact of k on SICQL’s performance, and Table 5 presents the few-shot evaluation returns of SICQL across representative environments with varying values of k . The results show that the performance of SICQL is not sensitive to k , with a moderate experience step of $k = 4$ performing the best in all evaluated domains. A small step may provide insufficient task-relevant information, limiting precise in-context inference. A large step may introduce redundancy and noise in the recent experience, and lead to overfitting during world model pretraining. Also, a large step will increase the computation load in pretraining the world model and decrease the speed in constructing the prompt for in-context task inference. In practice, a moderate value of k can achieve both fast and precise in-context inference, highlighting the superiority of our prompt design via world modeling.

Table 5: Few-shot results of SICQL’s performance with varying k on Mixed datasets.

K	Reach	Cheetah-Vel	Ant-Dir
2	802.00 ± 10.80	-37.51 ± 1.80	717.95 ± 37.81
4	806.97 ± 6.35	-35.48 ± 1.33	813.34 ± 14.12
6	794.19 ± 7.93	-40.36 ± 1.36	648.70 ± 56.75

5.5 Visualization Insights

We gain deep insights into the prompt construction process through t-SNE visualization on Cheetah-Vel and Ant-Dir tasks, as shown in Fig. 5. We use a continuous color spectrum to indicate task similarity. The initially entangled transitions are transformed into well-separated clusters in the prompt space, where points from different tasks are more clearly distinguished and similar tasks are grouped more closely. Further, prompt representations of Cheetah-Vel form a clear rectilinear distribution from blue (low velocity) to red (high velocity), exactly aligning with the rectilinear spectrum of target velocities *in a physical sense*. Similarly, prompt representations of Ant-Dir follow a cyclic spectrum that matches the periodicity of angular directions in a physical sense. This interesting finding highlights SICQL’s ability to distill meaningful task-specific information from raw transitions, enabling precise task inference to facilitate in-context learning capacity.

6 Conclusions, Limitations, and Future Work

In the paper, we propose SICQL, an innovative framework that introduces dynamic programming and world modeling to enable fundamental reward maximization and efficient task generalization in ICRL. SICQL employs a multi-head transformer to jointly predict optimal policies and in-context value functions, guided by a pretrained world model that encodes precise task-relevant information for efficient prompt construction. Policy improvement is achieved by fitting in-context value functions with expectile regression and distilling them into policy extraction via advantage-weighted regression, allowing for reward maximization while retaining the scalability and stability of supervised pretraining. Extensive evaluations verify the consistent superiority of SICQL over a range of competitive baselines.

Though, the length of our prompt is the same as the sampled transitions, which may not be short enough, especially for long-horizon interactive problems. Future work can explore extracting task information with more compact structures, e.g., encoding an episode or a skill into a single token. Another promising step is to leverage natural language as a higher-level task prompt for ICRL, harnessing a wealth of knowledge within pretrained language models.

References

- [1] David Ackley and Michael Littman. Generalization and scaling in reinforcement learning. In *Advances in Neural Information Processing Systems*, volume 2, 1989.
- [2] Robert Kirk, Amy Zhang, Edward Grefenstette, and Tim Rocktäschel. A survey of zero-shot generalisation in deep reinforcement learning. In *Journal of Artificial Intelligence Research*, volume 76, pages 201–264, 2023.
- [3] Josh Achiam, Steven Adler, Sandhini Agarwal, Lama Ahmad, Ilge Akkaya, Florencia Leoni Aleman, Diogo Almeida, Janko Altenschmidt, Sam Altman, Shyamal Anadkat, et al. GPT-4 technical report. *arXiv preprint arXiv:2303.08774*, 2023.
- [4] Daya Guo, Dejian Yang, Haowei Zhang, Junxiao Song, Ruoyu Zhang, et al. DeepSeek-R1: Incentivizing reasoning capability in LLMs via reinforcement learning. *arXiv preprint arXiv:2501.12948*, 2025.
- [5] Tom Brown, Benjamin Mann, Nick Ryder, Melanie Subbiah, Jared D Kaplan, Prafulla Dhariwal, Arvind Neelakantan, Pranav Shyam, Girish Sastry, Amanda Askell, et al. Language models are few-shot learners. In *Advances in Neural Information Processing Systems*, volume 33, pages 1877–1901, 2020.
- [6] Feng Li, Qing Jiang, Hao Zhang, Tianhe Ren, Shilong Liu, Xueyan Zou, Huaizhe Xu, Hongyang Li, Jianwei Yang, Chunyuan Li, et al. Visual in-context prompting. In *Proceedings of the IEEE/CVF Conference on Computer Vision and Pattern Recognition*, pages 12861–12871, 2024.
- [7] Zhendong Wang, Yifan Jiang, Yadong Lu, Pengcheng He, Weizhu Chen, Zhangyang Wang, Mingyuan Zhou, et al. In-context learning unlocked for diffusion models. In *Advances in Neural Information Processing Systems*, volume 36, pages 8542–8562, 2023.
- [8] Alexander Nikulin, Ilya Zisman, Alexey Zemtsov, and Vladislav Kurenkov. XLand-100B: A large-scale multi-task dataset for in-context reinforcement learning. In *Proceedings of International Conference on Learning Representations*, 2025.
- [9] Michael Laskin, Luyu Wang, Junhyuk Oh, Emilio Parisotto, Stephen Spencer, Richie Steigerwald, DJ Strouse, Steven Stenberg Hansen, Angelos Filos, Ethan Brooks, maxime gazeau, Himanshu Sahni, Satinder Singh, and Volodymyr Mnih. In-context reinforcement learning with algorithm distillation. In *Proceedings of International Conference on Learning Representations*, 2023.
- [10] Jonathan Lee, Annie Xie, Aldo Pacchiano, Yash Chandak, Chelsea Finn, Ofir Nachum, and Emma Brunskill. Supervised pretraining can learn in-context reinforcement learning. In *Advances in Neural Information Processing Systems*, volume 36, pages 43057–43083, 2023.
- [11] Licong Lin, Yu Bai, and Song Mei. Transformers as decision makers: Provable in-context reinforcement learning via supervised pretraining. In *Proceedings of International Conference on Learning Representations*, 2024.
- [12] Jaehyeon Son, Soochan Lee, and Gunhee Kim. Distilling reinforcement learning algorithms for in-context model-based planning. In *Proceedings of International Conference on Learning Representations*, 2025.
- [13] Sili Huang, Jifeng Hu, Hechang Chen, Lichao Sun, and Bo Yang. In-context decision transformer: Reinforcement learning via hierarchical chain-of-thought. In *Proceedings of International Conference on Machine Learning*, 2024.
- [14] Juncheng Dong, Moyang Guo, Ethan X Fang, Zhuoran Yang, and Vahid Tarokh. In-context reinforcement learning without optimal action labels. In *ICML 2024 Workshop on In-Context Learning*, 2024.
- [15] Viacheslav Sinii, Alexander Nikulin, Vladislav Kurenkov, Ilya Zisman, and Sergey Kolesnikov. In-context reinforcement learning for variable action spaces. In *Proceedings of International Conference on Machine Learning*, pages 45773–45793, 2024.

- [16] Denis Tarasov, Alexander Nikulin, Ilya Zisman, Albina Klepach, Andrei Polubarov, Lyubaykin Nikita, Alexander Derevyagin, Igor Kiselev, and Vladislav Kurenkov. Yes, Q-learning helps offline in-context RL. In *ICLR 2025 Workshop on Scalable Optimization for Efficient and Adaptive Foundation Models*, 2025.
- [17] Zhenwen Dai, Federico Tomasi, and Sina Ghiassian. In-context exploration-exploitation for reinforcement learning. In *Proceedings of International Conference on Learning Representations*, 2024.
- [18] David Silver, Satinder Singh, Doina Precup, and Richard S Sutton. Reward is enough. *Artificial Intelligence*, 299:103535, 2021.
- [19] Richard S Sutton, Andrew G Barto, et al. *Reinforcement learning: An introduction*, volume 1. MIT press Cambridge, 1998.
- [20] Taku Yamagata, Ahmed Khalil, and Raul Santos-Rodriguez. Q-learning decision transformer: Leveraging dynamic programming for conditional sequence modelling in offline RL. In *Proceedings of International Conference on Machine Learning*, pages 38989–39007, 2023.
- [21] Ioannis Kakogeorgiou, Spyros Gidaris, Bill Psomas, Yannis Avrithis, Andrei Bursuc, Konstantinos Karantzas, and Nikos Komodakis. What to hide from your students: Attention-guided masked image modeling. In *Proceedings of European Conference on Computer Vision*, pages 300–318, 2022.
- [22] Haoqi Yuan and Zongqing Lu. Robust task representations for offline meta-reinforcement learning via contrastive learning. In *Proceedings of International Conference on Machine Learning*, pages 25747–25759, 2022.
- [23] Danijar Hafner, Jurgis Pasukonis, Jimmy Ba, and Timothy Lillicrap. Mastering diverse control tasks through world models. *Nature*, pages 1–7, 2025.
- [24] Zhi Wang, Li Zhang, Wenhao Wu, Yuanheng Zhu, Dongbin Zhao, and Chunlin Chen. Meta-DT: Offline meta-RL as conditional sequence modeling with world model disentanglement. In *Advances in Neural Information Processing Systems*, volume 37, pages 44845–44870, 2024.
- [25] Yan Duan, John Schulman, Xi Chen, Peter L Bartlett, Ilya Sutskever, and Pieter Abbeel. RL²: Fast reinforcement learning via slow reinforcement learning. *arXiv preprint arXiv:1611.02779*, 2016.
- [26] Jake Grigsby, Linxi Fan, and Yuke Zhu. AMAGO: Scalable in-context reinforcement learning for adaptive agents. In *Proceedings of International Conference on Learning Representations*, 2024.
- [27] Jake Grigsby, Justin Sasek, Samyak Parajuli, Daniel Adeb, Amy Zhang, and Yuke Zhu. AMAGO-2: Breaking the multi-task barrier in meta-reinforcement learning with transformers. In *Advances in Neural Information Processing Systems*, volume 37, pages 87473–87508, 2024.
- [28] Chris Lu, Yannick Schroecker, Albert Gu, Emilio Parisotto, Jakob Foerster, Satinder Singh, and Feryal Behbahani. Structured state space models for in-context reinforcement learning. In *Advances in Neural Information Processing Systems*, volume 36, pages 47016–47031, 2023.
- [29] Ilya Zisman, Vladislav Kurenkov, Alexander Nikulin, Viacheslav Sini, and Sergey Kolesnikov. Emergence of in-context reinforcement learning from noise distillation. In *Proceedings of the International Conference on Machine Learning*, pages 62832–62846, 2024.
- [30] Anusha Nagabandi, Gregory Kahn, Ronald S Fearing, and Sergey Levine. Neural network dynamics for model-based deep reinforcement learning with model-free fine-tuning. In *IEEE International Conference on Robotics and Automation*, pages 7559–7566, 2018.
- [31] Yuri Burda, Harrison Edwards, Amos Storkey, and Oleg Klimov. Exploration by random network distillation. In *Proceedings of International Conference on Learning Representations*, 2019.

- [32] Luisa Zintgraf, Sebastian Schulze, Cong Lu, Leo Feng, Maximilian Igl, Kyriacos Shiarlis, Yarin Gal, Katja Hofmann, and Shimon Whiteson. VariBAD: Variational Bayes-adaptive deep RL via meta-learning. *The Journal of Machine Learning Research*, 22(1):13198–13236, 2021.
- [33] Fei Ni, Jianye Hao, Yao Mu, Yifu Yuan, Yan Zheng, Bin Wang, and Zhixuan Liang. MetaDiffuser: Diffusion model as conditional planner for offline meta-rl. In *Proceedings of International Conference on Machine Learning*, 2023.
- [34] Kimin Lee, Younggyo Seo, Seunghyun Lee, Honglak Lee, and Jinwoo Shin. Context-aware dynamics model for generalization in model-based reinforcement learning. In *Proceedings of International Conference on Machine Learning*, pages 5757–5766, 2020.
- [35] Ilya Kostrikov, Ashvin Nair, and Sergey Levine. Offline reinforcement learning with implicit Q-learning. In *Proceedings of International Conference on Learning Representations*, 2022.
- [36] Charlie Victor Snell, Ilya Kostrikov, Yi Su, Sherry Yang, and Sergey Levine. Offline RL for natural language generation with implicit language Q-learning. In *Proceedings of International Conference on Learning Representations*, 2023.
- [37] Xue Bin Peng, Aviral Kumar, Grace Zhang, and Sergey Levine. Advantage-weighted regression: Simple and scalable off-policy reinforcement learning. *arXiv preprint arXiv:1910.00177*, 2019.
- [38] Emanuel Todorov, Tom Erez, and Yuval Tassa. MuJoCo: A physics engine for model-based control. In *Proceedings of IEEE/RSJ International Conference on Intelligent Robots and Systems*, pages 5026–5033, 2012.
- [39] Tianhe Yu, Deirdre Quillen, Zhanpeng He, Ryan Julian, Karol Hausman, Chelsea Finn, and Sergey Levine. Meta-World: A benchmark and evaluation for multi-task and meta reinforcement learning. In *Conference on robot learning*, pages 1094–1100, 2020.
- [40] Tuomas Haarnoja, Aurick Zhou, Pieter Abbeel, and Sergey Levine. Soft actor-critic: Off-policy maximum entropy deep reinforcement learning with a stochastic actor. In *Proceedings of International Conference on Machine Learning*, pages 1861–1870, 2018.
- [41] John Schulman, Filip Wolski, Prafulla Dhariwal, Alec Radford, and Oleg Klimov. Proximal policy optimization algorithms. *arXiv preprint arXiv:1707.06347*, 2017.
- [42] Lanqing Li, Hai Zhang, Xinyu Zhang, Shatong Zhu, Yang YU, Junqiao Zhao, and Pheng-Ann Heng. Towards an information theoretic framework of context-based offline meta-reinforcement learning. In *Advances in Neural Information Processing Systems*, 2024.
- [43] Lanqing Li, Rui Yang, and Dijun Luo. FOCAL: Efficient fully-offline meta-reinforcement learning via distance metric learning and behavior regularization. In *Proceedings of International Conference on Learning Representations*, 2021.
- [44] Yunkai Gao, Rui Zhang, Jiaming Guo, Fan Wu, Qi Yi, Shaohui Peng, Siming Lan, Ruizhi Chen, Zidong Du, Xing Hu, et al. Context shift reduction for offline meta-reinforcement learning. In *Advances in Neural Information Processing Systems*, volume 36, pages 80024–80043, 2023.
- [45] Hao Liu and Pieter Abbeel. Emergent agentic transformer from chain of hindsight experience. In *Proceedings of International Conference on Machine Learning*, volume 202, pages 21362–21374, 2023.

A Limitations

Despite promising results, our approach has several limitations that warrant further investigation:

Prompt Length and Efficiency: Although the prompt length matches the sampled transitions, it may not be compact enough for long-horizon tasks, where increased complexity can cause inefficiencies. Future work should focus on condensing the prompt without losing key context.

Task Information Extraction: The current approach uses prompts equal in size to the sampled transitions, which works for short tasks but may not scale well for more complex ones. Using compact representations, like encoding episodes or skills into single tokens, could improve scalability.

Leveraging Natural Language for SICQL: A promising direction is using natural language as a higher-level prompt for SICQL. Pretrained language models could enhance knowledge transfer, improving generalization and adaptability, offering valuable opportunities for future research.

These limitations highlight critical areas for improvement, particularly in reducing prompt size and enhancing scalability for long-horizon tasks, offering valuable avenues for future research.

B Algorithm Pseudocodes

Based on the implementations presented in Sec. 4, this section provides an overview of the procedural steps of our method. Initially, Algorithm 1 outlines the pretraining process for the world model. Subsequently, Algorithm 2 describes the pipeline for training and testing SICQL.

Algorithm 1: Pretraining the World Model

Input: Training tasks M^{train} and corresponding offline datasets $\mathcal{D}^{\text{train}}$; Context encoder E_ϕ ; dynamics decoder D_φ ; Experience step k ;

for each iteration do

 Sample a task $M^i \sim M^{\text{train}}$ and obtain the corresponding dataset \mathcal{D}^i from $\mathcal{D}^{\text{train}}$
 Sample a transition tuple (s_t, a_t, r_t, s_{t+1}) with randomly selected t
 Obtain its h -step history $\eta_t^i = (s_{t-k}, a_{t-k}, r_{t-k}, \dots, s_{t-1}, a_{t-1}, r_{t-1}, s_t, a_t)$
 Compute the context $z_t^i = E_\phi(\eta_t^i)$
 Compute the predicted reward and next state $[\hat{r}_t, \hat{s}_{t+1}] = D_\varphi(s_t, a_t; z_t^i)$ Update E_ϕ and D_φ
 using the loss as $\mathcal{L}(\phi, \varphi) = \mathbb{E}_{\eta_t^i \sim M^i} \left[\mathbb{E}_{z_t^i \sim E_\phi(\eta_t^i)} \left[\left\| [r_t, s_{t+1}] - D_\varphi(s_t, a_t; z_t^i) \right\|^2 \right] \right]$

C The Details of Environments

DarkRoom: The agent is randomly placed in a 10×10 grid room, and the goal occupies one of the 100 grid cells. Thus, there are 100 possible goals. The agent’s observation is its current grid cell, i.e., $\mathcal{S} = [10] \times [10]$. At each step, the agent selects one of five actions: move up, down, left, right, or remain stationary. The agent receives a reward of 1 only upon reaching the goal and 0 otherwise. The episode horizon for Dark Room is 100. Consistent with [10], we use 80 of the 100 goals for pretraining and reserve the remaining 20 goals to test our model’s in-context RL capability on unseen tasks.

MuJoCo: The multi-task MuJoCo control testbed is a classical benchmark commonly used in continual RL, multi-task RL, and meta-RL. This testbed concludes two environments with reward function changes and one environment with transition dynamics changes as

- *Cheetah-Vel:* A planar cheetah must run forward at a specified target velocity along the positive x -axis. Each task is defined by a distinct reward function that penalizes the absolute deviation between the cheetah’s instantaneous velocity and its goal velocity. Goal velocities are drawn uniformly from $[0.1, 3.0]$, yielding a suite of tasks with varying targets.
- *Walker-Param:* A planar walker robot needs to move forward as fast as possible. Tasks differ in transition dynamics. For each task, the physical parameters of body mass, inertia, damping, and friction are randomized. The reward function is proportional to the running velocity in the positive

Algorithm 2: Scalable In-Context Q-Learning

Input: Training tasks M^{train} and corresponding offline datasets $\mathcal{D}^{\text{train}}$; Trained context encoder E_ϕ ; Transformer model parameterized by θ ; Prompt horizon h ;

\\ Pretraining model

for each iteration do

 Sample a task $M^i \sim M^{\text{train}}$ and obtain the corresponding dataset \mathcal{D}^i from $\mathcal{D}^{\text{train}}$

 Sample $(s_t^i, a_t^i, s_{t+1}^i, r_t^i)$ and a h -step trajectory $[s_1, a_1, r_1, \dots, s_h, a_h, r_h]^i$ randomly from dataset from \mathcal{D}^i .

 Use the trained context encoder E_ϕ to transform the h -step trajectory into lightweight prompt

$\beta^i := [z_1, \dots, z_h]^i = E_\phi([s_1, a_1, r_1, \dots, s_h, a_h, r_h]^i)$

\\ In-context values learning

 Update $V_\theta \leftarrow V_\theta - \rho \nabla_{V_\theta} L_V(\theta)$ using Eq. 5

 Update $Q_\theta \leftarrow Q_\theta - \rho \nabla_{Q_\theta} L_Q(\theta)$ using Eq. 4

 Update $\hat{\theta} \leftarrow (1 - \alpha)\hat{\theta} + \alpha\theta$

\\ In-context policy extraction

 Update $\pi_\theta \leftarrow \pi_\theta - \rho \nabla_{\pi_\theta} L_\pi(\theta)$ using Eq. 6

\\ Online test-time deployment

Sample unknown task $M^s \sim M^{\text{test}}$ and initialize empty $\beta = \{\}$.

for each episode in max_eps do

 Deploy π_θ by choosing $a_t \sim \pi_\theta(\cdot | s_t, \beta^t)$ at step t .

 Store (s_t, a_t, r_t, s_{t+1}) and use trained context encoder E_ϕ to transform the nearest h -step interactions into lightweight prompt β^t .

x-direction, which remains consistent for different tasks. The agent must therefore adapt its policy to diverse dynamics to achieve optimal performance.

- *Ant-Dir*: A quadrupedal ant robot must move in a specified direction. Each task defines a distinct target angle, and the reward is given by the cosine similarity between the agent’s velocity vector and the unit vector in the target direction. Target directions are drawn uniformly from $[0, 2\pi]$.

For all MuJoCo domains, we allocate 45 tasks for training and reserve the remaining 5 for evaluation, with each episode capped at 200 timesteps.

Meta-World: The Meta-Learning 1 (ML1) suite in Meta-World is a minimalist, single-task benchmark for few-shot meta-reinforcement learning. For each task, a Sawyer robotic arm in MuJoCo must reach a randomly Selected target—whose coordinates are withheld from observations—forcing the agent to infer the goal by trial and error. ML1’s sparse information and clear generalization challenge make it one of Meta-World’s most popular robotic manipulation testbeds for evaluating rapid adaptation in meta-RL.

- *Reach*: a Sawyer robotic arm must reach a randomly assigned goal position in 3D space, with each Reach task differing in goal location and reward function. The objective is to learn an optimal policy that efficiently generates the action sequence required to reach the specified target.
- *Push*: A Sawyer arm must push a block to a randomly placed target on a tabletop, with each task varying the block’s start position and corresponding reward function. Agents receive only sparse distance-based feedback and must infer the goal through interaction. This setup evaluates the agent’s ability to explore and adapt its pushing strategy under sparse supervision.

For all Meta-World domains, we allocate 45 tasks for training and reserve the remaining 5 for evaluation, with each episode capped at 100 timesteps.

D The Details of Dataset Construction

Pretraining Datasets for Darkroom: In the Dark Room environment, we gather 1,000 trajectories per task with horizon $H = 100$. At each step, we follow the optimal policy with probability ϵ and a random policy with probability $1 - \epsilon$. We choose ϵ so that the mean return of the pretraining datasets is below 40% of the optimal policy return, reflecting the challenging yet common scenarios.

Pretraining Datasets for MuJoCo and Meta-World: For each evaluation domain, we choose 45 tasks to construct the training datasets and train a single-task policy independently for each task. We use soft actor-critic (SAC) [40] for the MuJoCo domains. We use Proximal Policy Optimization (PPO) [41] for the Meta-World domain. We collect two types of offline datasets for each evaluation domain as

- *Mixed*: The dataset is constructed by mixing data from various policies, including those saved throughout the entire training process, offering a diverse range of experiences for training.
- *Medium*: The dataset is constructed using data from medium-quality policies, which, while suboptimal compared to high-quality policies, still offer valuable experiences for training.

Table 6 and Table 7 list the main hyperparameters for the SAC and PPO algorithms during offline data collection in all evaluation domains, respectively.

Table 6: Hyperparameters of SAC used to collect multi-task datasets.

Environments	Training steps	Warmup steps	Save frequency	Learning rate	Batch size	Soft update	Discount factor	Entropy ratio
Cheetah-Vel	500000	2000	10000	3e-4	256	0.005	0.99	0.2
Walker-Param	1000000	2000	10000	3e-4	256	0.005	0.99	0.2
Ant-dir	500000	2000	10000	3e-4	256	0.005	0.99	0.2

Table 7: Hyperparameters of PPO used to collect multi-task datasets.

Environments	Total_timesteps	n_steps	Learning_rate	Batch_size	n_epochs	Discount factor
Reach	400000	2048	3e-4	64	10	0.99
Push	1000000	2048	3e-4	64	10	0.99

E The Details of Baselines

This section presents seven representative baselines addressing the meta-task generalization problem, including one context-based offline meta-reinforcement learning (COMRL) method and six ICRL approaches. These baselines are thoughtfully selected to span the major domains of current offline meta-task research. Furthermore, since our proposed SICQL method belongs to the ICRL category, we incorporate more methods from this class as baselines for a comprehensive comparison. The detailed descriptions of these baselines are as follows:

- **IC-IQL** [16] extends standard ICRL by explicitly optimizing reinforcement learning objectives instead of relying solely on supervised losses as in AD. It augments AD with a Q-learning loss, where the value function is trained by updating both its head and the shared transformer backbone, while the policy is trained by updating only its own head.
- **DIT** [14] addresses the limitations of standard autoregressive imitation learning when trained on suboptimal trajectories. Instead of treating trajectory prediction purely as supervised learning, DIT emulates an actor-critic algorithm in-context by applying a weighted maximum likelihood estimation (WMLE) loss, where the weights are directly computed from observed rewards.

- **DICP** [12], combines model-based reinforcement learning with prior in-context RL approaches such as AD and IDT. DICP leverages a pre-trained Transformer not only to condition past transitions but also to simulate future trajectories and estimate long-term returns, enabling proactive decision-making without parameter updates. DICP jointly models environment dynamics and policy improvements in context, resulting in greater adaptability and sample efficiency, particularly in long-horizon tasks.
- **IDT** [13], employs a hierarchical learning framework that decomposes decision-making across temporal scales to address the high computational cost of prior in-context RL methods on long-horizon tasks. Its architecture consists of three modules: (i) Decision-Making, which predicts high-level decisions; (ii) Decision-to-Go, which decodes these decisions into low-level actions; and (iii) Decision-Review, which maps low-level actions back to high-level representations. Built upon a transformer architecture similar to that of AD, IDT addresses complex decision-making in long-horizon tasks while reducing computational costs through hierarchical modeling.
- **AD** [9], casts in-context RL as a supervised sequence-modeling task: a causal Transformer is pretrained on across-episodic trajectories covering the entire RL learning to predict subsequent actions, thereby emulating standard RL update dynamics without explicit gradient updates. In AD, trajectories gathered across episodes are organized into fixed-length sequences of length H , with each trajectory tokenized as an interleaved series of states, actions, and rewards. This allows the model to learn purely from contextual information, enabling in-context adaptation of policies to new tasks.
- **DPT** [10], adopts a supervised training paradigm to enable in-context learning for RL tasks. The core idea is to train a transformer to predict the provided optimal action for a given query state purely based on context, using interaction histories from diverse tasks as in-context datasets. DPT treats each transition tuple (s, a, s', r) as a single token, rather than decomposing it into separate embeddings. This allows the attention mechanism to directly model relationships between full transitions, preserving the structural and semantic integrity of the interaction data.
- **UNICORN** [42], integrates representative methods such as FOCAL [43], CORRO [22], and CSRO [44], this work proposes a unified information-theoretic framework that interprets these approaches as optimizing different approximation bounds of the mutual information between task variables and their latent representations. Building on the information bottleneck principle, it further derives a general and unified objective for task representation learning, facilitating the extraction of robust and transferable task representations. This method provides a unified information-theoretic perspective that summarizes and connects several mainstream context-based offline meta-RL approaches. As it integrates key ideas from representative COMRL algorithms, it can serve as a strong and generalizable baseline.

Mainstream ICRL algorithms predominantly rely on imitation learning paradigms, which tend to learn suboptimal behaviors when pretraining data is limited in size or quality. To ensure fair comparison, we standardize the dataset size and quality across methods during pretraining. In our task setting, AD struggles to extract effective policy improvement operators due to insufficient offline data. Therefore, we adopt an AD variant that incorporates a reward-based trajectory sorting mechanism from AT [45] to better distill policy improvements. Additionally, since UNICORN under the COMRL setting requires warm-up data for task representation inference, we align it with the ICRL setup by initializing task representations using randomly sampled trajectories and updating them after each episode.

F Implementation Details of SICQL

World Model. In this paper, we adopt streamlined architectures for each component of the world model: the context encoder, and the dynamics decoder. The context encoder first employs a fully connected multi-layer perceptron (MLP) followed by a gated recurrent unit (GRU) network, both using ReLU activations. The GRU processes the agent’s k step history $\eta_t^i = (s_{t-k}, a_{t-k}, r_{t-k}, \dots, s_{t-1}, a_{t-1}, r_{t-1}, s_t, a_t)^i$. and produces a 128-dimensional hidden vector. This vector is then projected via the MLP into a 16-dimensional task representation z_t^i . The reward decoder is an MLP that receives the tuple $(s_t^i, a_t^i, s_{t+1}^i, z_t^i)$ and passes it through two hidden layers of size 128 to predict the scalar reward \hat{r}_t^i . Analogously, the state transition decoder is an MLP that takes (s_t^i, a_t^i, z_t^i) as input and uses two 128-dimensional hidden layers to predict the next state \hat{s}_{t+1}^i .

Table 8: The network configurations used for SICQL.

World Model	Value	Causal Transformer	Value
GRU hidden dim	128	Layers num	4
Prompt representation dim	16	Attention heads num	1
Decoder hidden dim	128	Activation function	ReLU
Decoder hidden layers num	2		
Activation function	ReLU		

Table 9: Hyperparameters of SICQL on various domains.

Hyperparameters	Darkroom	Push	Reach	Cheetah-Vel	Walker-Param	Ant-Dir
Training steps	200000	400000	400000	400000	400000	400000
Learning rate	3e-4	1e-4	1e-4	3e-4	3e-4	3e-4
Prompt horizon h	100	100	100	200	200	200
Embedding dim	32	128	128	128	128	128
Output layers num	1	2	2	2	2	2
Temperature parameter λ	0.01	0.001	0.001	0.001	0.1	0.01
Expectile parameter ω	0.7	0.5	0.5	0.7	0.7	0.7
Soft updat α	0.005	0.005	0.005	0.005	0.005 e	0.005
Discount factor	0.99	0.99	0.99	0.99	0.99	0.99

Causal Transformer. We implement SICQL on top of the official DPT codebase released by DPT [10] (<https://github.com/jon-lee/decision-pretrained-transformer>). We adhere to their architectural design, and construct the embeddings for the GPT-2 backbone as follows. Specifically, given a task dataset \mathcal{D}^i , we sample $(s_t^i, a_t^i, s_{t+1}^i, r_t^i)$ and a h -step trajectory $[s_1, a_1, r_1, \dots, s_h, a_h, r_h]^i$ randomly from dataset from \mathcal{D}^i . Then we use the pretrained context encoder E_ϕ to transform raw transitions in this trajectory into precise and lightweight prompt $\beta^i := [z_1, \dots, z_h]^i = E_\phi([s_1, a_1, r_1, \dots, s_h, a_h, r_h]^i)$. We form state vectors $\xi_{s_t}^i = (s_t^i, 0)$, next state vectors $\xi_{s_{t+1}}^i = (s_{t+1}^i, 0)$ and state-action vectors $\xi_{\{sa\}_t}^i = (s_t^i, a_t^i, 0)$ by concatenating the relevant quantities and padding with zeros so that each ξ^i has dimension $d_\xi := 2d_S + d_A + 1$. The $(h+1)$ -length sequence is given by $X = (\xi^i, z_1^i, \dots, z_h^i)$. We first apply linear projection $\text{Linear}(\cdot)$ to each vector and outputs the sequence $Y = (\hat{y}_0, \hat{y}_1, \dots, \hat{y}_h)$. Then the $(h+1)$ -length tokens are fed into the transformer and predict output autoregressively using a causal self-attention mask. In the output layer, we employ separate linear layers to produce the actions, the state-values, and the Q-values, respectively. In summary, Table 8 shows the details of network structures.

Algorithm Hyperparameters. We evaluate the proposed SICQL algorithm on six environments: Darkroom, Push, Reach, Cheetah-Vel, Walker-Param, and Ant-Dir. For all experiments, we use the Adam optimizer with a weight decay of 1e-4, gradient-norm clipping at 10, an experience step of 4, and a batch size of 128. Table 9 summarizes the detailed hyperparameters of SICQL in each domain.

Compute. We train our models on NVIDIA RTX3090 GPUs paired with an AMD EPYC 9654 CPU and 512GB of RAM. Pretraining the world model takes approximately 0.2–2 hours, while pretraining the causal transformer requires about 1–12 hours, depending on the environment’s complexity.

G Graphic Results for Hyperparameter Analysis

Due to limited space, we only present tabular results in Sec. 5.4 in the main text. Here, we present the corresponding graphic results. Figure 6 shows the few-shot evaluation return curves of SICQL on Mixed datasets with varying values of λ . Figure 7 presents few-shot evaluation return curves of SICQL on Mixed datasets with varying values of k .

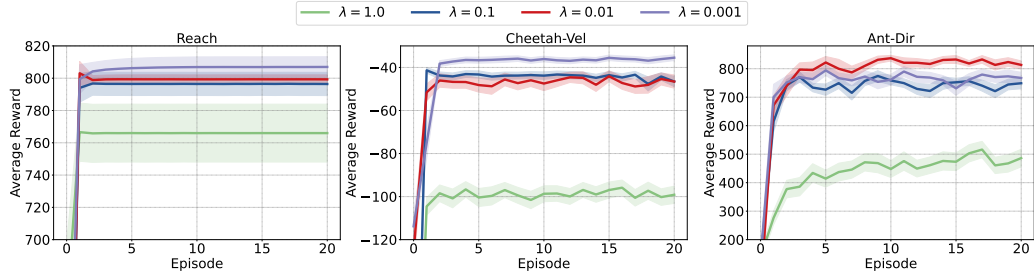


Figure 6: Few-shot evaluation return curves of SICQL on Mixed datasets with varying values of λ .

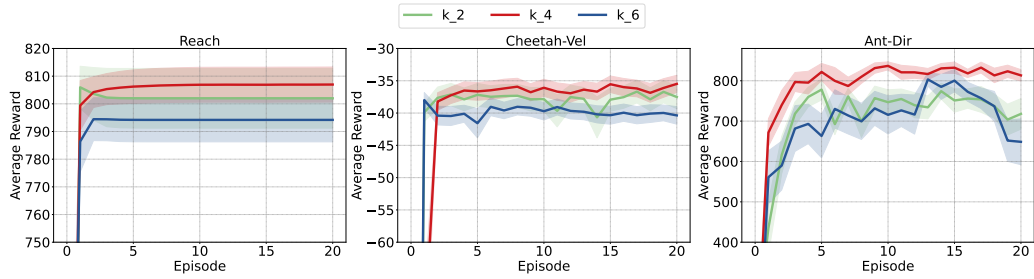


Figure 7: Few-shot evaluation return curves of SICQL on Mixed datasets with varying values of k .